Morphology Evolution of Non-toxic $MA_3Bi_2I_9$ Based Lead Free Perovskite Solar Cells

Ashish KULKARNI, IKEGAMI Masashi and MIYASAKA Tsutomu

Graduate School of Engineering, Toin University of Yokohama

（2017 年 3 月 18 日　受理）

***Abstract* — Lead halide perovskites have gained tremendous research attention due to its high power conversion efficiency (PCE) but its poor stability and lead-toxicity stands as a major obstacle for commercialization. Bismuth based lead-free perovskite material ($MA_3Bi_2I_9$) have shown better long term stability but the efficiency is far behind those of lead. This present review summarizes the morphology studies that have been carried out and further directs the research towards achieving high efficiency for $MA_3Bi_2I_9$ perovskite materials.**

I. Introduction

Organic-inorganic hybrid lead (Pb) halide perovskite solar cells (PSCs) are currently witnessing the fastest growth in photovoltaic technologies compare to already established one. Ever since the pioneering work from our group, organic-inorganic hybrid lead halide perovskite solar cells (PSCs) have witnessed unprecedented rise from 3.8 % to certified 22% power conversion efficiency (PCE).[1), 2), 3)] Perovskite material having a general formula of AMX_3 (A = $CH_3NH_3^+$ (MA); M = Pb^{2+}; X = I^-, Br^-) forms a cubic structure in which the metal Pb locates itself at the center of an octahedral $[MX_6]^{4-}$ unit while the A cation resides at the eight corners of cubic shell as shown in ***Figure 1***. Also, the structure AMX_3 must satisfy the tolerance factor *t* ($t = (R_A+R_M)/\sqrt{2}\,(R_X+R_M)$) where R_A, R_M, R_X corresponds to the ionic radii of A, M and X respectively. For cubic structure, the ideal value for *t* is 1. Many studies have focused on the replacement of $CH_3NH_3^+$ (MA) with $CH(NH_2)_{2+}$ (FA), cesium (Cs^+), mixture of FA/Cs, FA/MA/Cs, FA/MA/Cs/Rb to satisfy the tolerance factor and form stable 3D perovskite structure with suitable composition, high durability, and augmented efficiency. In addition to cost-effective simple solution processibility, lead perovskite possess number of remarkable optoelectronic properties such as direct band gap of ~1.6 eV, high absorption coefficient (5 x 10^4 cm^{-1}), awfully sharp absorption onset, long diffusion length as long as 1μm, less

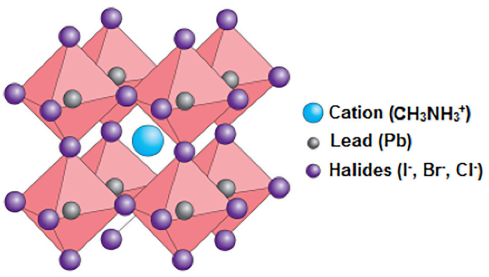

Fig. 1 Perovskite crystal structure.

Ashish KULKARNI, IKEGAMI Masashi and MIYASAKA Tsutomu
Graduate School of Engineering, Toin University of Yokohama. 1614 Kurogane-cho, Aoba-ku, Yokohama 225-8503, Japan

electron and hole effective masses, photon recycling capability, to name few.[4]

Despite of several advantages lead based perovskites suffers from long term stability issue. The cation A (from AMX_3) gets eliminate from the perovskite structure with exposure to moisture, prolonged illumination under sun-light in air and/or with heating leaving behind the degraded product lead iodide (PbI_2). Long-term durability up to several hours to several months, in research laboratories, has been achieved by modifying UV-sensitive TiO_2 layer with MgO layer,[5] by replacing TiO_2 with SnO_2,[6] interfacial modification [7] to name few, but durability to several tens of years still remains a big challenge. Development of robust encapsulation strategies can help the perovskite module to last long. However lead toxicity stands as a major obstacle in a way to commercialization. It is reported that exposure of lead to human can be catastrophic effecting nervous and reproductive systems.[7] This undesired lead toxicity issue, regardless of high efficiency, motivated the research community to pave a new path towards the development of lead-free eco-friendly perovskite materials.

Tin (Sn) based perovskites have been demonstrated as the first step to address the lead toxicity issue with initial efficiency of 5.7% and now scaled up to ~6.4% in pure Sn and ~15% in Pb-Sn mix perovskite. Even though Sn perovskites have shown promising optoelectronic properties such as long diffusion length, superior electron mobility (~2000 $cm^2 V^{-1} s^{-1}$),[9] narrow optical band gap and bulk n-type electrical conductivity (5 x 10^{-2} S cm^{-1}), Sn perovskite gets oxidizes in its +4 stable oxidation state, from +2, when exposed to ambient air and due to this unstable oxidation state the device fabrication has to be carried out in inert atmosphere. Moreover, reports have shown that Sn perovskite can be even more toxic than lead perovskite, by releasing high amount of hydroiodic acid (HI) in to the environment as a byproduct than its counter-parts.[8), 10)]

Lately, Group 15 metals, antimony (Sb) and bismuth (Bi) based perovskite have been theoretically and experimentally investigated. Sitting in the neighborhood of Pb, Sb and Bi possess similar electronic configuration and comparable ionic radii with that of Pb allowing them to incorporate effectively into the perovskite lattice. This further lead to explore the possibilities of heterovalent substitution of Pb^{2+} by incorporating trivalent metals (Bi, Sb) in combination of monovalent metals such as silver (Ag), gold (Au), copper (Cu), potassium (K) into the perovskite structure forming double perovskites possessing molecular structure of $A_2MM'X_6$, A = Cs^+, MA^+; M = Bi^{3+}, Sb^{3+}; M' = Ag^+, Au^+, Cu^+, K^+; X = I^-, Cl^-, Br^-. Among many combinations of double perovskite materials, $Cs_2BiAgBr_6$ and $Cs_2BiAgCl_6$ were explored earnestly. Slavney *et al*. synthesized $Cs_2BiAgBr_6$ which exhibited an indirect band gap of 1.95 eV and reported strong photoluminescence in the visible region and long recombination lifetime of 660 ns similar to that of $MAPbI_3$. McClure *et al*. synthesized both Br and Cl based materials ($Cs_2BiAgBr_6$ and $Cs_2BiAgCl_6$) and reported the band gap of 2.19 eV and 2.77 eV respectively obtained from diffuse reflectance spectroscopy and DFT calculations. Even though attempts have shown that double perovskites based on Ag-Bi combination can be a promising replacement for lead perovskites[8] recently Savory *et al*. reported its limitations to achieve high PCE (maximum limit is 10%), owing to its wide indirect band gap and large carrier effective masses. Theoretical investigation suggests that this limitation can be overcome by replacing Ag with indium (In) or thallium (Tl) and the Bi-In and Bi-Tl based double perovskite material possess direct band gap of around ~2 eV. Unfortunately, in addition to wide band gap (~2 eV) which is not suitable for photovoltaic applications, the higher toxicity of Tl limits its further use.[11]

The present mini review summarizes recent

efforts and developments of non-toxic bismuth based lead free perovskite materials, other than double perovskites, and their applications in photovoltaic devices. Ternary non-toxic metal halides based perovskite materials ($A_3M_2X_9$; A = Cs^+, MA^+, Rb^+; M = Bi^{3+}, Sb^{3+}; X = I^-, Cl^-) have emerged recently as potential candidate due to its non-toxicity and high moisture stability. Optical properties, crystal structure, dielectric studies and quantum physical properties of various ternary bismuth halide perovskite materials have been formerly investigated but attempts to use it in photovoltaic devices was lately addressed. Firstly, Park *et al*. integrated three different ternary bismuth halide absorbers; $Cs_3Bi_2I_9$, $MA_3Bi_2I_9$ and $MA_3Bi_2I_{9-x}Cl_x$, with optical band gap of 2.2, 2.1, and 2.4 eV respectively, into photovoltaic devices and achieved 1%, 0.1% and 0.03% for $Cs_3Bi_2I_9$, $MA_3Bi_2I_9$ and $MA_3Bi_2I_{9-x}Cl_x$ respectively. Poor interconnected thin dendrite like layer and high exciton binding energy (70–300 meV) was the reason believed for low efficiency. Hoye *et al*. deposited $MA_3Bi_2I_9$ by conventional 2-step solution and by vapour processed deposition and systematically studied its crystal structure, optoelectronic properties and stability. Phase pure $MA_3Bi_2I_9$ showed indirect band gap of 2.04 eV which is closed to the value reported by park *et al*. They also reported and compared long term stability of $MA_3Bi_2I_9$ with $MAPbI_3$ by exposing both films to relative humidity of 61%. The colour of $MAPbI_3$ changed from brown to yellow in 5 days while $MA_3Bi_2I_9$ maintained its colour even after 13 days and showed slightly bright colour after 26 days which was accounted for the formation of Bi_2O_3 or BiOI layer on the surface demonstrating a promising long term stability of $MA_3Bi_2I_9$ photovoltaic absorber. Moreover, vapour processed film exhibited characteristic PL decay times over 0.76 ns, with bulk lifetime possibly close to 0.56 ns which further indicated its promising application in photovoltaic devices.

Oz *et al*. first reported $MA_3Bi_2I_9$ in planar architecture with PEDOT:PSS and PCBM as hole and electron transporting material respectively. Interestingly with PEDOT:PSS under layer, the $MA_3Bi_2I_9$ layer showed island like morphology with hexagonal shaped crystals with an average size of ~1–2 μm and in the cross-section SEM image, they observed that the thickness of $MA_3Bi_2I_9$ varied from 80 nm to 150 nm signifying its inhomogeneous layer. In contrast to previous reports, they reported bathochromic shift of the excitonic absorption band ($\Delta = 0.06$) which indicates less localized exciton states and further reported its band gap and exciton binding energy to be 2.94 eV and 400 meV, respectively.[11]

II. Morphological evolution of $MA_3Bi_2I_9$

Change in morphology with the effect of underlayer, as mentioned above, motivated us to study the effect of different TiO_2 electron transporting scaffold layer *i.e.* TiO_2 anatase, TiO_2 brookite mesoporous and planar architecture, on

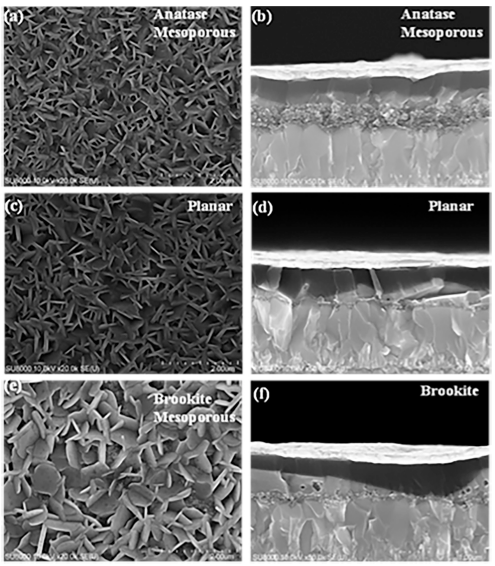

Fig. 2 Top and cross-section SEM images of $MA_3Bi_2I_9$ on (a, b) anatase mesoporous, (c, d) planar architecture, (e, f) brookite mesoporous layer.

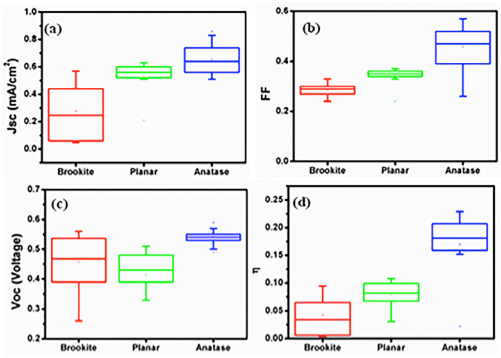

Fig. 3 Device parameters with different device architectures.

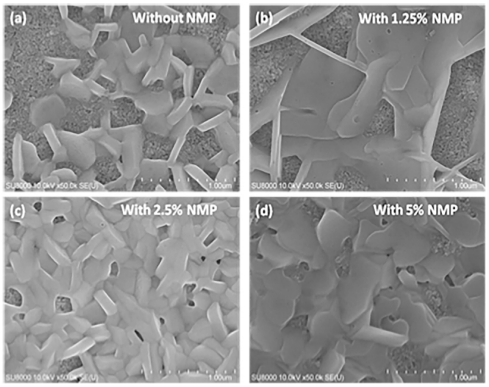

Fig. 4 Top surface SEM images of $MA_3Bi_2I_9$ perovskites without (a) and with different concentration of NMP (b, c, d).

the morphology and photovoltaic performance of $MA_3Bi_2I_9$. Surface coverage of $MA_3Bi_2I_9$ on planar and anatase TiO_2 were slightly similar and better than on brookite TiO_2 mesoporous layer coated substrates as shown in ***Figure 2***. Also, in case of brookite TiO_2 under layer, $MA_3Bi_2I_9$ showed large interconnected crystals compared to planar and anatase TiO_2 mesoporous under layer. Cross-section SEM image revealed that in case of brookite TiO_2 under layer the perovskite layer does not form a uniform capping layer allowing HTM layer to touch the mesoporous layer and similarly in case of planar architecture, $MA_3Bi_2I_9$ layer showed slightly non-uniform perovskite capping layer. However, in case of anatase TiO_2 mesoporous architecture uniform perovskite capping layer was seen. Large interconnected crystals, in case of brookite TiO_2 under layer, was attributed to strong inter-necking of brookite TiO_2 particles leading to poor infiltration and fast crystallization of $MA_3Bi_2I_9$. This significantly evidences the effect of under layer on the morphological property of $MA_3Bi_2I_9$. Further we reported crystal structure of $MA_3Bi_2I_9$ which was resolved into *P63/mmc* space group and was in consistent with the prior reports. Devices were fabricated by integrating various ETL and sandwiching $MA_3Bi_2I_9$ between ETL and HTL and as expected device with anatase mesoporous under layer showed better photovoltaic performance in comparison to planar and brookite TiO_2 under layer based cells. The device metrics for best performing mesoporous TiO_2 based device were: short-circuit current (J_{sc}) = 0.86 mA/cm^2, open-circuit voltage (V_{oc}) = 0.56 V, fill factor (FF) = 0.48 and PCE = 0.259%. Important correlation between various device parameters of the studied device architecture was observed and is shown here in ***Figure 3***. According to prior reports $MA_3Bi_2I_9$ possess high charge carrier density of ~10^{16} cm^{-3}, [13] was the reason accounted for low efficiency in addition to poor morphology and suitable neighboring charge collecting layers.[14]

To address the morphological issue we further directed our work by introducing *N*-methyl-2-pyrrolidone (NMP) as a morphology controller into the $MA_3Bi_2I_9$-DMF solution. Addition of NMP slowed down the evaporation rate during the spin coating and heating process as the colour of the substrate changed from transparent to orange, in contrast to non-NMP based system which maintained orange colour throughout the complete process. This clearly signified the change in morphology which was evidently observed in SEM images. Morphology was highly affected with change in different concentration of NMP and with 2.5% of NMP additive, the $MA_3Bi_2I_9$ showed uniform coverage over TiO_2 mesoporous coated substrates as shown in ***Figure 4***. From the XRD

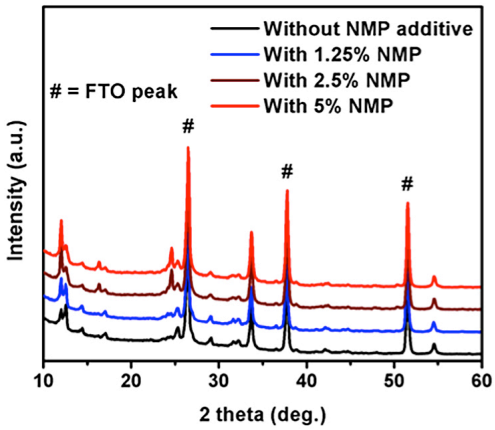

Fig. 5 XRD pattern of $MA_3Bi_2I_9$ layer without and with different concentration of NMP on mesoporous TiO_2 coated FTO substrates.

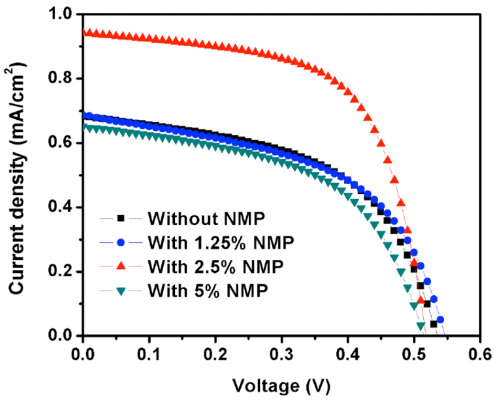

Fig. 6 Best performing device J-V curve without and with different concentration of NMP.

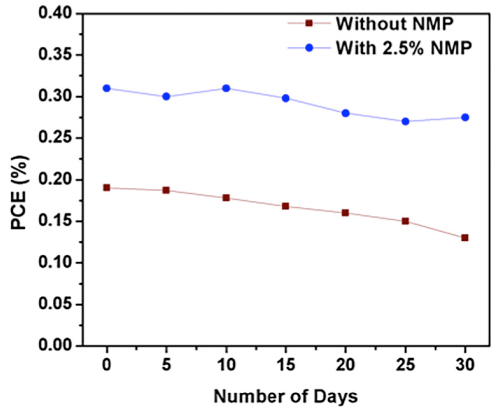

Fig. 7 Long term stability of device without and with NMP additive under relative humidity of 60%.

pattern we observed that the intensity of peak at 2θ = ~12° and 24° increases with the addition of NMP. This indicated that poor crystallinity of $MA_3Bi_2I_9$ on mesoporous TiO_2 was improved with the addition of NMP (***Figure 5***). Devices were fabricated and measured to verify the effect of tuned morphology on photovoltaic performance. Due to better coverage device with 2.5% NMP showed improvement in J_{sc} and device performance. Best performing device showed 0.31% efficiency compared to other NMP concentration and non-NMP case which showed 0.18% as shown in ***Figure 6***. There was slight hysteresis observed in the device J-V curve which can be attributed to interface of $MA_3Bi_2I_9$ and its neighboring charge collecting layers.[15] Interestingly the NMP additive device, after exposing them to relative humidity of 60%, showed better long term stability compared to non-additive system (***Figure 7***) due to its high crystallinity and stable oxidation state of Bi. This also suggests the choice of suitable ETL for $MA_3Bi_2I_9$ which can help to enhance its crystallinity, J_{sc} and device performance.[16] Moreover, in this work we concluded that tuning the morphology does not help to improve the efficiency much and tuning the intrinsic optoelectronic property is the way to enhance the efficiency of lead-free bismuth based ternary halides perovskite solar cells. This further directs research towards doping or adding additives to reduce the intrinsic carrier densities and/or tune the band gap of $MA_3Bi_2I_9$ which can further enhance the efficiency of lead free perovskite solar cells. Continuation of this review with summarization of more worldwide recent trends and developments in ternary bismuth/antimony halides and other group 15 metal based perovskite materials is under progress and will be submitted for publication soon.

III. Conclusion and outlook

In this review article, we provided an overview of progress in lead perovskite solar cells and its limitations for commercialization followed by progress in lead-free perovskite. Also, we discussed about the effect of electron transporting layer and high boiling point solvent additive on the morphology of $MA_3Bi_2I_9$. Towards the end we directed towards enhancement in PCE of bismuth based lead-free perovskite solar cells.

[References]

1) Kojima A, Teshima K Shirai Y, Miyasaka T, (2009) Organometal halide perovskites as visible-light sensitizers for photovoltaic cells. *J. Am. Chem. Soc.*, 131: 6050–6051.
2) Miyasaka T, (2015) Perovskite Photovoltaics: Rare Functions of Organo Lead Halide in Solar Cells and Optoelectronic Devices. *Chem. Lett.*, 44: 720–729.
3) Best solar cell efficiency chart. Available at http://www.nrel.gov/ncpv/images/efficiency_chart.jpg accessed on (14th March 2017).
4) Singh T, Singh J, Miyasaka T, (2016) Role of Metal Oxide Electron-Transport Layer Modification on the Stability of High Performing Perovskite Solar Cells. *ChemSusChem*, 9: 2559–2566.
5) Kulkarni A, Jena A, Chen H-W, Sanehira Y, Ikegami M, Miyasaka T, (2016) Revealing and Reducing Possible Recombination Losses Within Compact Layer by Incorporating MgO Layer in Perovskite Solar Cells. *Solar Energy*, 136: 379–384.
6) Pinpithak P, Chen H-W, Kulkarni A, Sanehira Y, Ikegami M, Miyasaka T, (2017) Low-Temperature and Ambient Air Processes of Amorphous SnOx-based Mixed Halide Perovskite Planar Solar Cell. *Chem Lett.*, 46: 382–384.
7) Chaudhary B, Kulkarni A, Jena A. K, Ikegami M, Udagawa Y, Kunigita H, Ema K, Miyasaka T, (2017) Poly(4-vinylpyridine)-based interfacial passivation to enhace voltage and moisture stability of lead halide perovskite solar cells. *ChemSusChem*, DOI: 10.1002/cssc.2001700271.
8) Babayigit A, Ethirajan A, Muller M, Conings B, (2016) Toxicity of organometal halide perovskite solar cells. *Nature Materials*, 15: 247-251.
9) Stoumpos CC, Malliakas CD, Kanatzidis MG, (2013) Semiconducting Tin and Lead Iodide Perovskites with Organic Cations: Phase Transitions, High Mobilities and Near-Infrared Photoluminescent Properties. *Inorg. Chem.*, 52: 9019-9038.
10) Giustino F, Snaith HJ, (2016) Towards Lead-Free Perovskite Solar Cells. *ACS Energy Lett.*, 1: 1233-1240.
11) Savory CN, Walsh A, Scanlon DO, (2016) Can Pb-Free Halide Double Perovskites Support High-Efficiency Solar Cells?. *ACS Energy Lett.*, 1: 949–955.
12) Hoefler SF, Trimmel G, Rath T, (2017) Progress on Lead-Free Metal Halide Perovskites for Photovoltaic Applications: A Review. *Monatsh Chem.*, DOI: 10.1007/s00706-017-1933-9.
13) Lyu M, Yun J-H, Cai M, Jiao Y, Bernhardt PV, Zhang M, Wang Q, Aijun D, Wang H, Liu G, Wang L, (2016) Organic-Inorganic Bismuth (III)-based Material: A Lead-free, Air-stable and Solution-processable Light-absorber Beyond Organolead Perovskites. *Nano Research*, 9 (3): 692–702.
14) Singh T, Kulkarni A, Ikegami M, Miyasaka T, (2016) Effect of Electron Transporting Layer on Bismuth-Based Lead-Free Perovskite $(CH_3NH_3)_3$ Bi_2I_9 for Photovoltaic Applications. *ACS Appl. Mater. Interfaces*, 8 (23): 14542–14547.
15) Jena A, Kulkarni A, Ikegami M, Miyasaka T, (2016) Steady state performance, photo-induced performance degradation and their relation to transient hysteresis in perovskite solar cells. *Journal of Power Sources*, 309: 1–10.
16) Kulkarni A, Singh T, Ikegami M, Miyasaka T, (2017) Photovoltaic enhancement of bismuth halide hybrid perovskite by N-methyl pyrrolidone-assisted morphology conversion. *RSC Adv.*, 7: 9456–9460.